Scientific paper

Radical Scavenging Activity: DFT and Multilinear Regression Studies of Benzofuran-1,3-thiazolidin-4-one Derivatives

Fella Ati^{1,2}, Soraya Abtouche¹, Boubekeur Maouche¹ and Meziane Brahimi^{1,*}

¹ Laboratory of Theoretical and Physical Chemistry and Informatics Chemistry (LPCTCI), University of Sciences and Technology Houari Boumediene. (USTHB). BP N° 32 Al alia, 16111, Algiers. Algeria.

² Department of Chemistry, Faculty of Sciences, Saad Dahlab University, BLIDA 1, Algiers, Algeria.

* Corresponding author: E-mail: mez_brahimi@yahoo.fr; m.brahimi@usthb.dz

Received: 08-24-2024

Abstract

The free radical scavenging activity of benzofuran Schiff base and thiazolidinone derivatives has been investigated using the density functional theory (DFT) calculations. Three primary mechanisms were developed: sequential proton loss electron transfer (SPLET), single electron transfer followed by proton transfer (SET-PT), and hydrogen atom transfer (HAT). Several thermodynamic descriptors were computed in both gas and solvent phases at the B3LYP/6-311G and 6-311G (d, p) level of theory. Our findings suggest that compounds **3a**, **3c**, **3f**, **4d**, and **4e** may scavenge free radicals through one of these three pathways. The results indicate that SPLET is favored in polar environments, while HAT is the thermodynamically preferred mechanism in the gas phase and non-polar solutions. Electron-withdrawing groups (EWG) attached to the π conjugated system at the N position of the benzofuran derivatives decrease bond dissociation enthalpies (BDE), while electron-donating groups (EDGs) are helpful to decrease the ionization potentials (IPs). The results of the multilinear regression statistical analyses indicate a good correlation between the IC₅₀ and ionization potential, in addition to the proton dissociation enthalpy, proton affinity, and the electron transfer enthalpy descriptors.

Keywords: Benzofuran, thiazolidinone derivatives; Antioxidant activity; DFT, MLR.

1. Introduction

Reactive oxygen species (ROS) and reactive nitrogen species (RNS) are the by-products of the cellular redox process and are well documented to play a dual role, acting as both harmful and beneficial species. Overproduction of these species leads to oxidative stress, a state in which the biological system is unable to ensure the oxidant-antioxidant equilibrium.1 Oxidative stress, causes irreversible damage to cells, lipids, membranes, proteins, and DNA. It is also implicated in premature aging and major diseases, including Alzheimer's disease, autism, cancer, HIV infection, and cerebrovascular accidents.^{2,3} In a normal physiological environment, the reactive species generation is closely regulated by various non-enzymatic and enzymatic antioxidants. Antioxidants are substances that can scavenge free radicals by donating an electron or a hydrogen atom, chelating redox-active metals and inhibiting lipoxygenases. A,5 To search for new antioxidants, benzofuran is one of the most important heterocyclic containing oxygen. Many benzofuran derivatives, such as benzofuran 1,3-thiazolidin-4-ones exhibit potent biological and pharmacological activities, like anti-Alzheimer's, anti-dermal, anti-hyperglycemic, anti-inflammatory, β -adrenoceptor antagonistic, anti-microbial, anti-pyretic, anti-tumor, immunosuppressive, and especially antiviral activities, 12,13 They also demonstrate anthelmintic, anti-histaminic, anti-hyperlipidemic, anti-bacterial, anti-convulsant, anti-proliferative, anti-tubercular, anti-diabetic, anti-fungal, cardiovascular, follicle-stimulating hormone receptor agonist, hypnotic activities, as reported in several research article, 14-16 and anti-viral activities is also observed. 17-20

The synthesis of benzofuran-azo, benzofuran-thiazole, benzofuran-hydrazo, and benzofuran-piperazine hybrids as new antitumor benzofuran agents,²¹ and

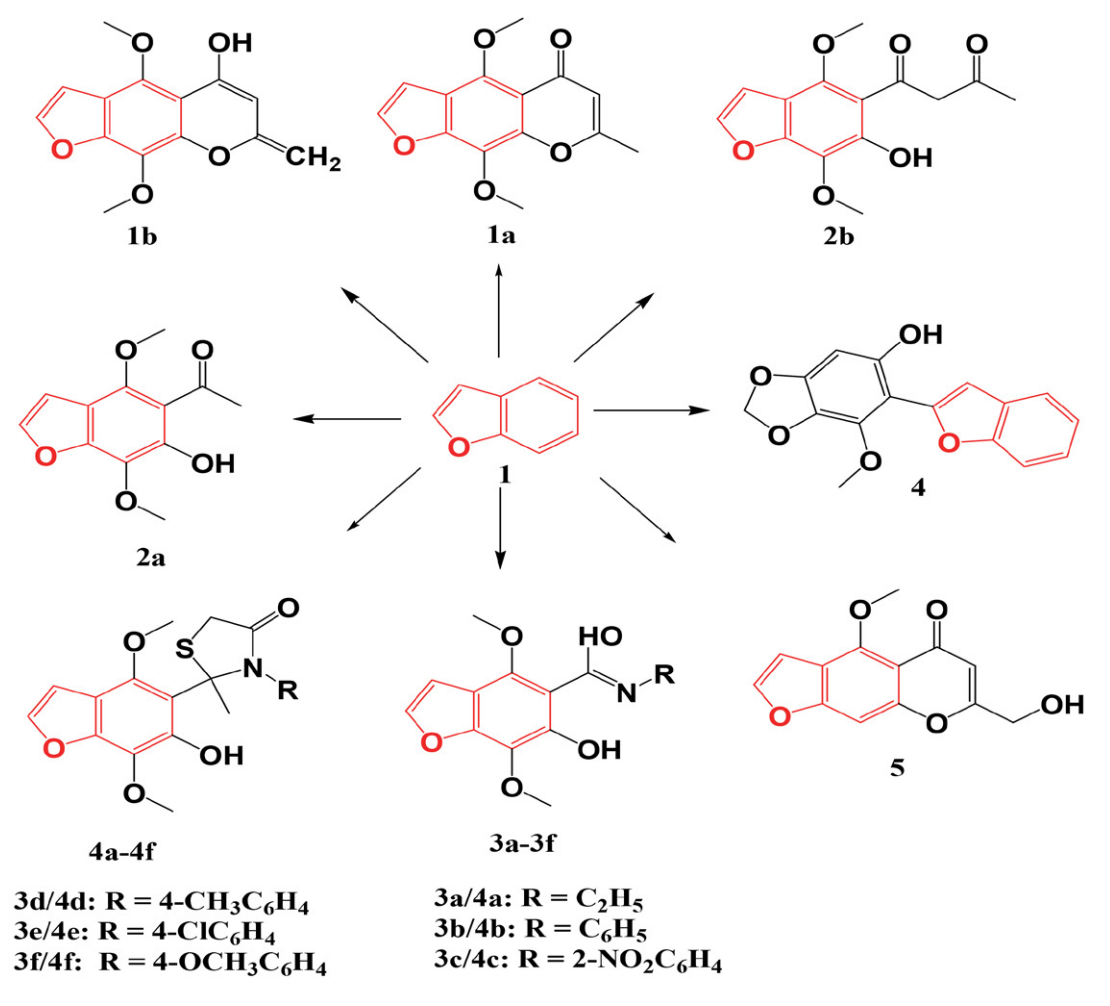


Figure 1: Structures of the studied benzofuran derivatives.

the synthesis of bis(benzofuran–thiazolidinone) and bis(benzofuran–thiazinanone) as Chikungunya virus inhibiting agents continues to be areas of active research. Iminosubstituted (3a-3f) and 1,3-thiazolidinone (4a-4f) substituted benzofuran derivatives (see Figure 1) were recently screened for radical scavenging activity using the 2,2-diphenyl-1-picrylhydrazyl (DPPH) Assay. The initial results indicate that khellin (1a) and its hydrolyzed derivatives (2a, 2b) exhibit low antioxidant activity, whereas the 1,3-benzofuran derivatives (3c, 3d, 3f) and (4d) demonstrate comparable antioxidant activity with EC₅₀ values of 10.59, 9.72, 8.57 and 8.27 μ M respectively. These values approach that of the standard drug Trolox (5.42 μ M).

In this work, we aim to develop a theoretical model of the antioxidant activity of benzofuran-derivatives,²⁵ to help researchers in understanding this phenomenon and designing novel antioxidant drugs. For this purpose, we calculated the BDE, IP, PDE, PA, ETE, frontier molecular orbital (HOMO, LUMO), and spin density of radicals parameters are calculated to investigate the free radical scavenging mechanism.

2. Computational Method

Gaussian09 software was used for all calculations. ²⁶ The geometries optimization and vibrational normal modes calculations were performed at the density functional theory (DFT) level using the B3LYP functional, ^{27,28} with the 6-311G, and 6-311G(d, p) basis sets, in both gas and solvated phases. Unrestricted calculations were performed for open-shell systems such as radical species. Solvent effects (water, benzene, and DMSO) were taken into account using the self-consistent reaction field polarized continuum model (SCRF-PCM). ^{29,30}

The ADME properties are calculated with ADMET-lab $2.0,^{31}$ and bioactivity studies are evaluated with Molinspiration online property calculation toolkit. To determine the most relevant descriptors of the antioxidant activity represented by the IC₅₀, a multilinear regression analysis was performed using Excel. In the literature, three fundamental antioxidant mechanisms are proposed and widely discussed such as HAT, eq. (I)), SET-PT, eq. (II), and SPLET, eq. (III).

$$ArOH + R^* = ArO^* + RH \tag{I}$$

$$ArOH + R^* = ArOH^{*+} + R^-$$
 (II)

$$ArOH = ArO^{-} + H^{+}$$
 (IIIa)

$$ArO^- + R^* = ArO^* + R^- \tag{IIIb}$$

$$R^- + H^+ = + RH \tag{IIIc}$$

The physicochemical parameters BDE, IP, PDE, PA, and ETE were calculated using the following formulas.³⁵

$$BDE = H(ArO^*) + H(H^*) - H(ArOH)$$
 (1)

$$IP = H(ArOH^{*+}) + H(e^{-}) - H(ArOH)$$
 (2)

$$PDE = H(ArO^*) + H(H^+) - H(ArOH^{*+})$$
 (3)

$$PA = H(ArO^{-}) + H(H^{+}) - H(ArOH)$$
 (4)

$$ETE = H(ArO^*) + H(e^-) - H(ArO^-)$$
(5)

where H(X) is the sum of electronic and thermal enthalpies of the X species.³

3. Results and Discussion

3. 1. HAT Mechanism

The O-H BDE appeared as a most significant descriptor to evaluate the structure-activity relationships in

antioxidants.³⁶ It is also closely associated with the SET-PT and SPLET mechanisms. This associations arises the total energy requirements for the (SET-PT, IP+PDE) and (SPLET, PA+ETE) mechanisms are strongly correlated with the BDE value (see Figure 2).³⁷

As shown in Table 1, Khellin (1a, keto form) is inactive due to the absence of OH group (see Figure 3), and the large BDEs of C_5 -H in phenyl ring (113.07 kcal/mol) and BDEs of C_7 -H (86.72 kcal/mol). This is in agreement with the experimental results.²³

Figure 3: keto-enol tautomeric equilibrium.

The gas phase HOMO energies are – 5.71 eV for **1a** (keto form) and – 5.44 eV for **1b** (enol form). The BDE of the enol form is lower than that of Trolox by 64.13 kcal/mol. For compound **1a**, the difference is of the order of 6 (keto form), and 22 (enol form) kcal/mol, indicating that **1b** has greater hydrogen atom mobility. Furthermore, the

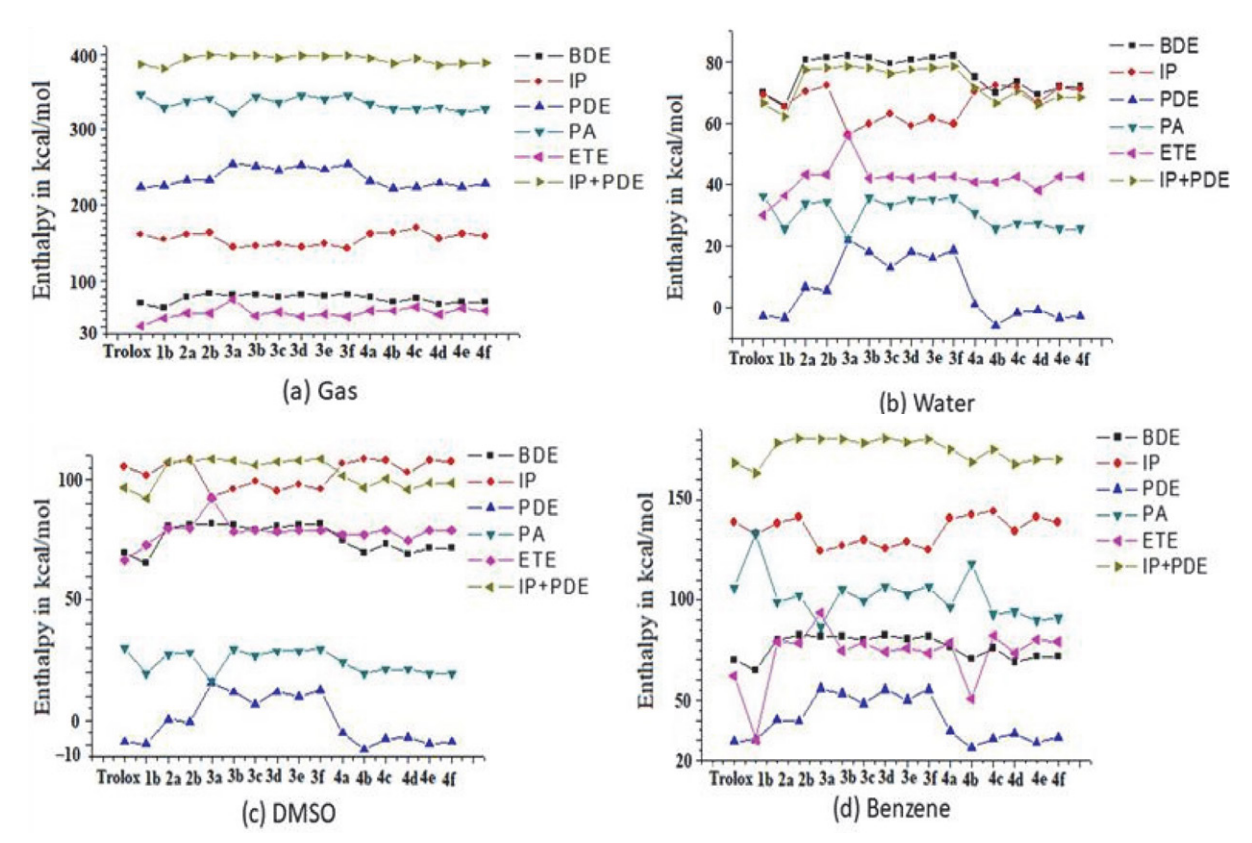


Figure 2: Calculated enthalpies graphics ((a) in gas, (b) in water, (c) in DMSO, and (d) in benzene at B3LYP/6-311G level.

Table 1: Theoretical properties of khellin (1a).

Theoretical properties	Gas-phase	Water	DMSO	Benzene
$BDE(C_5-H)$	113.07	113.70	113.70	113.07
$BDE(C_7-H)$	86.72	87.35	87.35	86.72
IP (kcal/mol)	158.25	69.03	105.39	136.79
PDE (kcal/mol)	244.35	15.06	8.78	48.31
$E_{HOMO}(eV)$	- 5.71	- 5.98	- 5.97	- 5.85
$E_{LUMO}(eV)$	- 1.47	- 1.72	- 1.72	- 1.57

gas phase IP values for **1a** and **1b** are 158.25 kcal/mol and 155.2 kcal/mol, respectively. So, all calculations show that **1b** is more nucleophilic than **1a** and thus the enol form is more reactive than the keto form.

The O-H benzofuran derivatives BDEs values, in the gas and solvate phase, are listed in Table 2. For the two hydrolyzed derivatives of khellin **2a** and **2b**, the BDEs are 79.19 kcal/mol and 82.95 kcal/mol, respectively. These values are higher than that of Trolox by about 9 and 12.5 kcal/mol, respectively. Thus, **2a** and **2b** have less ability to donate protons than Trolox.

These BDEs values of benzofuran Schiff base derivatives in gas phase, illustrated in Table 2, are in the range of 79.19–82.33 kcal/mol which is higher than those of benzofuran thiazolidinone derivatives (69.78–78.56 kcal/mol). This indicates that benzofuran thiazolidinone derivatives are more potent antioxidants than benzofuran Schiff base derivatives. Polarization leads to the same order of BDEs in a solvated medium, however in the gas state, there is an inversion between the positions of molecules **3c** and **4d**, respectively. The B3LYP/6-311G(d, p) level leads to the same conclusions with a relative error of the order of 3.9

kcal/mol (in gas) and of the order of 4.4 kcal/mol in water, DMSO and benzene.

The order of the BDEs of the series (3a to 3f), in the gas phase, is 3b = 3d = 3f > 3a > 3e > 3c. Therefore, their H-donating abilities are in reverse order. In water and DMSO solvents, these BDEs values follow the same order of 3c > 3d > 3b = 3e > 3a = 3f. Among the studied benzofuran derivatives, 3c is the most active independently of the media, while 3f is the less one. The difference between calculated and experimental BDEs (23) is around 2 kcal/mol. This difference likely due to the different steric effects present in the molecules during the attack of the DPPH radical, 38,39 unlike Trolox.

Benzofuran derivatives structures analysis shows that intramolecular hydrogen bonding (IHB) can be established between the O-H group and the neighboring C=N.⁴⁰ The bond length O-H and N...H in gas and water are listed in Table 3.

Table 3: Hydrogen bonds O-H...N (in Å) for the benzofuran Shiff base derivatives in gas and in water.

Compo- und	d _{O-H} in Gas	d _{O-H} in Water	$\begin{array}{c} d_NH \\ \text{in Gas} \end{array}$	$\begin{array}{c} d_{N}{H} \\ \text{in Water} \end{array}$	Angle (O-HN)
3c	1.01	1.02	1.62	1.59	147.14
3e	1.02	1.03	1.60	1.55	147.26
3b	1.02	1.04	1.59	1.54	147.55
3d	1.02	1.04	1.59	1.53	147.69
3f	1.02	1.04	1.59	1.53	147.61
3a	1.03	1.06	1.57	1.48	148.48

The ranking of BDE values (3c > 3e > 3a > 3b = 3d = 3f, Table 3) is inverse to the strength of the hydrogen bond

Table 2: Calculated BDE values (kcal/mol) in the gas, and different solvents for the studied benzofuran derivatives at the B3LYP/6-311G level. The values obtained at the B3LYP/6-311G(d,p) level are given in parenthesis.

Compounds [23]	BDE in Gas	BDE in Water	BDE in DMSO	BDE in Benzene	IC ₅₀ (μM)
Trolox	70.41(71.59)	69.78(71.07)	69.78(71.07)	69.78(71.23)	5.42
1b	64.13	65.39	65.39	64.76	/
2a	79.19	80.45	80.45	79.82	/
2b	82.95	81.07	81.07	82.33	/
3a	81.70	81.70	81.70	81.70	/
3b	82.33	81.07	81.07	81.07	/
3c	79.19(64.53)	79.19(78.90)	79.19(78.92)	79.82(79.46)	10.59
3d	82.33(82.30)	80.45(80.45)	80.45(80.50)	82.33(81.61)	9.72
3e	81.07	81.07	81.07	80.45	/
3f	82.33(82.51)	81.70(80.71)	81.70(80.75)	81.70(81.82)	8.57
4a	78.56	74.80	74.80	76.68	/
4b	71.66	69.78	69.78	70.41	/
4c	77.93	73.54	73.54	76.05	/
4d	69.78	69.15	69.15	69.15	8.27
4e	71.66	71.66	71.66	71.66	/
4f	72.29	71.66	71.66	71.66	/

which becomes increasingly shorter compared to the sum of the Van der Waals radii involved in it.⁴⁰ The variation in hydrogen bond lengths is the same in the gas and hydrate phase except for compound $\bf 3a$ which has a different structure with the absence of the phenyl group attached to N. It can be concluded that for these benzofuran derivatives, electron-withdrawing Groups (EWG) attached to π conjugated groups at the N position of the Schiff base decrease significantly the BDEs ($\bf 3c$ and $\bf 3e$). By contrast, electron-donating groups (EDG) increase significantly the BDEs ($\bf 3d$ and $\bf 3f$).

The BDEs order, in the gas phase, is 4a > 4c > 4f > 4e= 4b > 4d, for the series (4a to 4f). Thus, their H-donating abilities are in reverse order. The same order is observed in all solvents. Accordingly, 4d is predicted to be the most active among the benzofuran thiazolidinone derivatives studied independently of the medium, while **4a** is the least one.

These results are in agreement with the experiment.²³ The BDE of 4d (69.78kcal/mol in gas) is lower than that of Trolox by about 0.63 kcal/mol at the B3LYP/6-311G level of theory, and about 1.85kcal/mol at B3LYP/6-311G (d, p) level of theory. This result indicates that 4d possesses antioxidant properties comparable to those of Trolox. The observed order of antioxidant activity, 4d > 4b = 4e > 4f > 4c > 4a, can be attributed to the intramolecular hydrogen bond (IHB) formed between the phenolic hydrogen and the oxygen atom of the -O-CH₃ group in compound 4a, 4c. In compounds 4b, 4d, 4e, and 4f, the IHB may involve the phenolic hydrogen and the neighboring C-N group (in 4b) or the neighboring C-S group (in 4d, 4e, and 4f) as depicted in Figure 4.

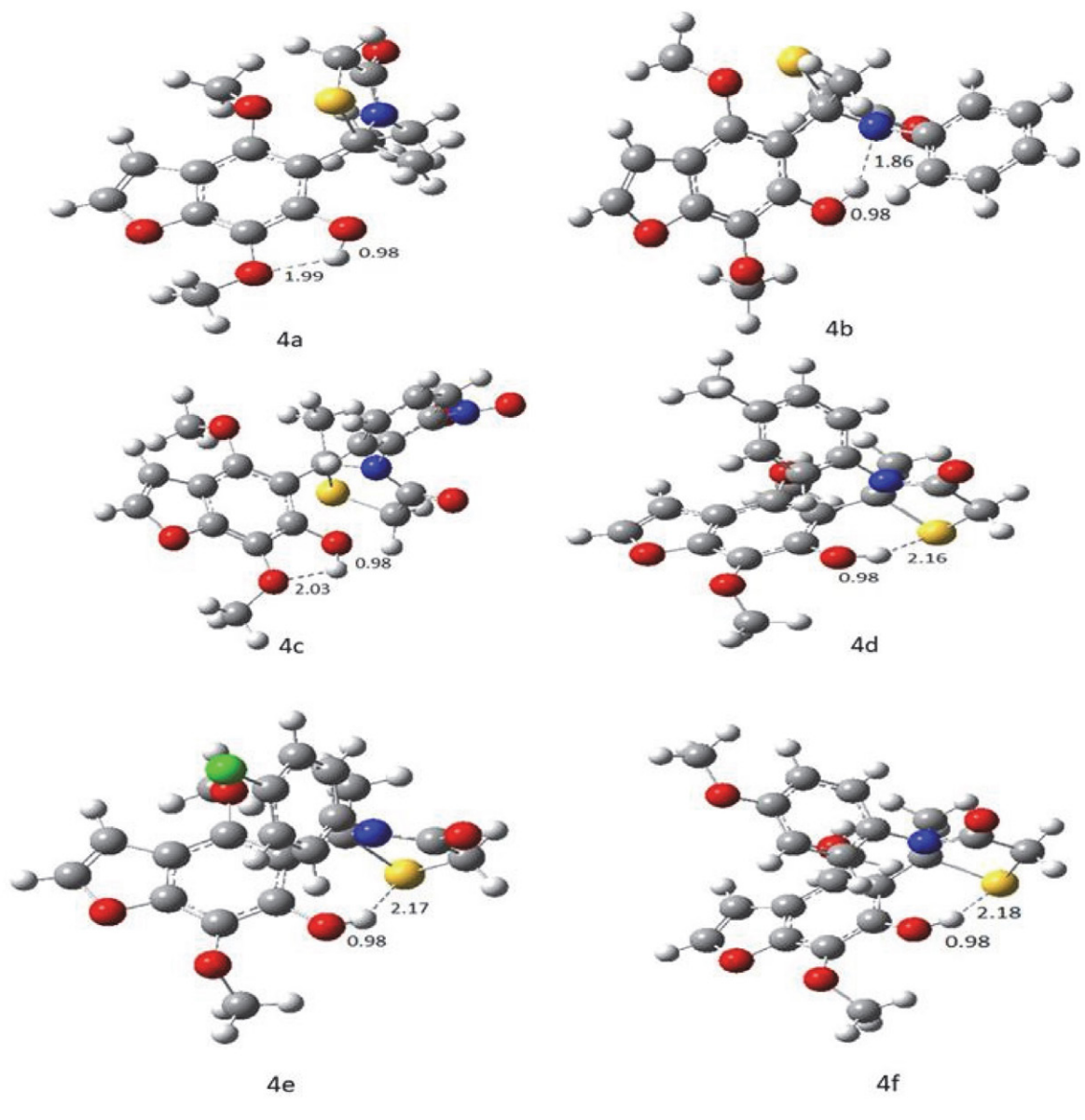


Figure 4: IHB in benzofuran thiazolidinone derivatives.

Figure 5: Spin density distribution of phenoxy radicals of the benzofuran derivatives.

Compound **4a** exhibits the highest BDE (see Table 2) due to its phenolic hydrogen is involved in a strong IHB with the oxygen of the -O-CH₃ group. Consequently, the high BDE arises from the fact that the hydrogen atom elimination necessitates the rupture of the IHB. **4d** displays the lowest value because its hydrogen is involved in a weak IHB with the C-S group. The slight variation in bond dissociation energies across different solvents is owing to the absence of charged species in the HAT process.

The spin densities of all the studied benzofuran derivatives (Figure 5) are distributed over the phenolic oxygen atom and the benzofuran ring. Analysis of these spin densities insights into the difference in reactivity of the hydroxyl (-OH) group, as reflected in their BDE values. Greater delocalization of the radical's spin density generally indicates easier radical formation and lower BDE value. 41

The spin densities of the oxygen atom are similar to that of benzofuran Schiff base derivatives (0.404). In **3c**, the spin density is substantially lower (0.392), resulting in lower BDEs for **3c**. This can explain why these radicals have similar BDE and experimental results. Furthermore, it can be concluded that the different substituents at the N position do not affect the spin density distribution. For benzofuran thiazolidinone derivatives, **4d** exhibits the lowest spin density (0.302), while **4b** display the highest one (0.376). **4d** possesses the lowest BDE value among all the others.

3. 2. SET-PT Mechanism

In addition to their implication in the HAT mechanism, phenolic compounds can also scavenge free radicals through single electron. The calculated IP and PDE involved in the SET-PT mechanism in different environment are reported in supplementary materials (see Tables S-1a, 1b, 1c, and 1d).

In gas phase, the IPs values classification for the (3a-3f) series are classified as follows: 3f < 3a < 3d < 3b < 3c < 3e. In benzene solvent the order is 3a < 3f < 3d < 3b < 3e < 3c. These variations likely arise from the small energy differences between 3f and 3a and between 3c and 3e which does not exceed 1.25kcal/mol. In water and DMSO, the IPs follows the same order: 3a < 3d < 3b = 3f < 3e < 3c. Compounds 3f and 3a exhibit the strongest electron donating ability in the gas and solvated mediums, while 3c and 3e are the lowest ones.

For the series (4a to 4f), the order of the IP values is 4d < 4f < 4a = 4e < 4b < 4c in all media (see Tables S-1a, 1b, 1c and 1d). These results indicate that 4d is the most electron-donor than the others in all cases defined in Table S-1, while 4c has the lowest ones. These coherent predictions are generally in agreement with the results that can be deduced from the HOMO energies reported in Table 4.

A comparison of the IPs of **3b** and **3f** reveals that the first value is smaller than the second by about 2.5 kcal/mol.

Table 4: HOMO and LUMO energies for the studied benzofuran derivatives at the B3LYP /6-311G, and 6-311G(d, p) level.

Compounds	E _{HOMO} (eV)	E_{LUMO} (eV)
1b	- 5.44	-1.41
3a	- 5.59	- 1.39
3b	- 5.59	- 1.71
3c	- 5.75(- 5.62)	-3.59(-2.90)
3d	- 5.55(- 5.46)	- 1.65(- 1.37)
3e	- 5.72	- 1.94
3f	- 5.53(- 5.42)	- 1.61(- 1.31)
4a	- 5.82	- 0.90
4b	- 5.83	- 1.28
4c	- 6.12	- 2.82
4d	- 5.72	- 0.75
4e	- 6.06	- 0.67
4f	- 5.90	- 1.12

This shows that when an electron-donating group (EDG) is introduced, thereby enhancing the electron-donor ability of the benzofuran derivatives. The same trend is observed for 4b and 4d. In contrast to the BDEs values, the IPs obtained in a solvated medium, are significantly lower compared to those in gas phase. This can be attributed to the stabilization of charged species in polar solvents.⁴² As an example the IP value, of the most active compound 3f, decreases by 84kcal/mol when passing from gas to a hydrated state. These results show the important role of solvent polarity in controlling the SET-PT mechanism. Compound 3a has the highest PDE values in each medium, while 4d has the smallest value, and 4b appears to be the most active in the deprotonation step. Notable solvent effects on the PDEs values are observed since the cationic radical and the proton are charged species. Deprotonation is easier, particularly in polar solvents such as water and DMSO.As shown in supplementary materials (see Tables S-1a, b, c and d), the PIs values obtained for all the benzofuran derivatives [56.47 to 170.18 kcal/mol] are, for the most part, lower than those of Trolox [69.03 to 161.39 kcal/ mol]. This suggests that the benzofuran derivatives studied have EDG ability greater than that of Trolox.

3. 3. SPLET Mechanism

SPLET mechanism has been reported as a possible pathway to trap radicals, particularly in polar environments. For the (3a to 3f) series, the data analysis of Tables 4a, b, c, and d reveals that the order of the AP values is consistent across all the environments defined in the same Tables, 3a < 3c < 3e < 3b < 3d = 3f. For the series (4a to 4f), the order is 4e < 4b = 4c = 4f < 4d < 4a. These findings suggest that 3a and 4e are more susceptible to deprotonation compared to the others compounds.

The PAs values comparison of compounds **3b** and **3e** shows that the first value is smaller than the second one by about 4.4kcal/mol, demonstrating that the effect of the

electron-withdrawing Group (EWG) diminishes the PAs values and improves deprotonation. This observation also holds true for **4b** and **4e**. We also observe notable solvent effects on the values of the APs (see Tables S-1a, 1b, 1c, and 1d in supplementary materials). For example, PA value of **3a** decreases from 322.16 (in the gas) to 86.59 (in benzene), 22.59 (in water), and 16.31 kcal/mol (in DMSO), which is probably due to the higher solvation enthalpy of the proton. This implies that polar solvents favor the deprotonation of the studied species. The PA values of the studied benzofurans are significantly lower than that of reference (Trolox). Thus, the deprotonation of the compounds is easier than for Trolox.

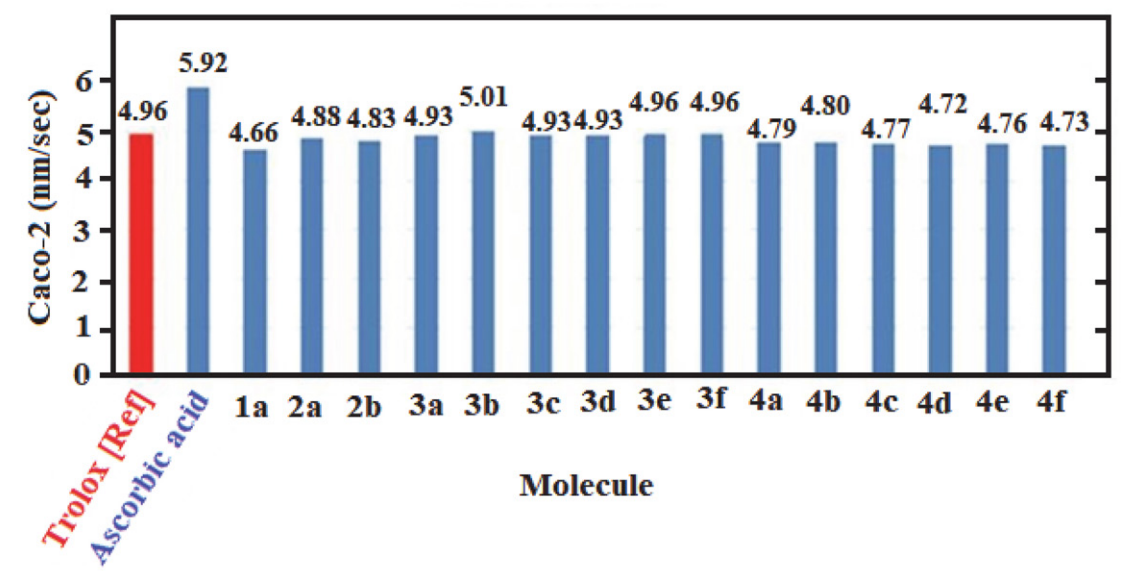
3. 4. ADME Properties of Studied Compounds

ADME properties (predicting absorption, distribution, metabolism, and excretion) of new drug candidates are critical to identify molecules with undesirable drug-like profiles. A drug in blood exists in two forms, bounded and unbounded. A portion of the drug binds to plasma protein, while the other part being unbound. The unbound form is being metabolized and/or excreted from the body whereas the bound part will be released to maintain equilibrium. The fraction unbound is the active fraction and can be excreted. These fore, plasma protein binding (PPB%) is an important pharmacokinetic factor, ⁴³ a compound is classified as strongly bound if PPB % > 90% which can lead to a low therapeutic index (reduces its action as well as its efficacy).

On the other hand, predicting human intestinal absorption (HIA %) of the drug is crucial important to identifying the potential drug candidate. HIA is generally considered the sum of bioavailability and absorption often evaluated from ration or cumulative excretion in urine,

bile, and excrement. ⁴⁴ For a given compound, HIA% values that occur, in the range [0 to 0.3], indicate poor, in [0.3 to 0.7] average, and [0.7 to 1.0] good intestinal absorption. Furthermore, blood-brain barrier (BBB) penetration is an important pharmaceutical criterion. BBB penetration is presented as the concentration ratio of steady-state or radio-labeled compounds in a brain (C_{brain}) and peripheral blood (C_{blood}). Compounds that can pass the BBB are called central nervous system active (CNS-active) compounds (BBB > 0.30), while those that are unable are called CNS-inactive compounds (BBB < 0.30).

The human colon adenocarcinoma cell lines (Caco-2) as an alternative approach for the human intestinal epithelium, commonly used to estimate in vivo drug permeability due to their morphological and functional similarities. Compounds with a caco-2 value < -5.15 (logcm/s) are lower permeable and those with a value > -5.15(logcm/s) are considered highly permeable and able to penetrate cellular biochemical processes.⁴⁵ Furthermore, the apparent permeability coefficient (Papp) of the MDCK (Martin-Darby Canine Kidney) cell lines is also used to evaluate the effect of the BBB index. An MDCK permeability value of less than 2.10⁻⁶ cm/s indicates that the compounds are low permeability, a value between [2 and 20.10⁻⁶] cm/s indicates that the compounds are moderately permeable and value greater than 20.10⁻⁶ cm/s indicates that the compounds have high MDCK permeability.⁴⁶ Thus, the Caco-2 and MDCK indexes are important for the eligibility of a drug candidate. The main drug targets are receptors, ion channels, nucleic acid, and transporters. So, the values of calculation of ion channel modulation (ICM), nuclear receptor ligand (NRL), bioactivity for G protein-coupled receptors ligand (GPCR) enzyme, and kinase inhibition (EI) and (KI) respectively indicate binding affinity of the species to the receptors and enzymes. A negative value means low affinity, while positive value shows



Histogram 1: Caco-2cell permeability index as vs. compounds.

greater affinity.⁴⁷ The logarithm of the n-octanol/water partition coefficient (log P), is important and has an impact both one membrane permeability and on hydrophobic binding to macromolecules. Compounds with values in the range [0 to 3] (log mol/l) will be considered as good candidates. Finally, the logarithm of the aqueous solubility value (log S) is a good index that quantifies the absorption of the drug and its disintegration by its dissolution. It is of great importance in drug discovery. Compounds having values in the range [–4 to 0.5] log(mol/l) will be considered as good drug candidates.

Table 2, given in supplementary materials, shows that compounds **1a**, **2a**, **2b**, **3a**, and **4a** have, (log S) values of between –3.19 and –3,585 which correspond to molecules with good dissolution, and (log P) values of between 1,877 and 2.563 which correspond to good permeability and hydrophobic binding of these compound to macromolecules.

The analysis of predicted ADME properties (see Tables S-2a and b) of the studied compounds revealed the *in vivo* BBB penetration efficiency ranging from 0.028 to 0.501 cm/s. Compounds **3a**, **4a**, and **4c** ensure their level of CNS activity compared to Trolox or ascorbic acid with 0.153 and 0.073 respectively. The values of Caco-2 cell permeability values ranged from -5.012 to -4.659 (nm/sec). All the studied compounds exhibited high permeability, as Caco-2 cell permeability values exceeding -5.15 (log(c-m)/s) are generally considered indicative of high permeability (see histogram 1 and Tables S-2a and 2b).

This efficiency provides sustained permeability to bind with the plasma proteins. The PPB affinity values are in the range of 72.28 to 100.2%. Compounds 1a, 2a, 2b, and 3a have PPB affinity < 90% indicating that may be

efficient. In contrast, compounds **3b-3f** and **4a-4f** have % PPB > 90% so, they may have a low therapeutic index (see histogram 2 and Tables S-2a and 2b).

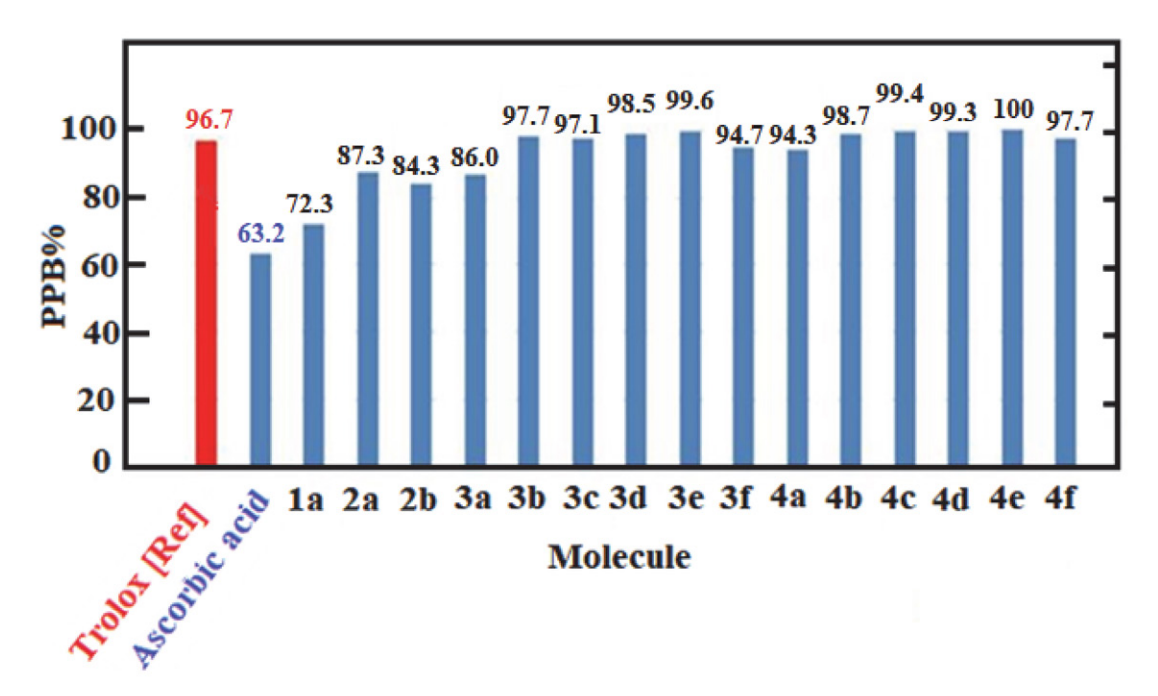
The MDCK cell permeability identified for them is ranging from $0.9.10^{-5}$ to $3.0.10^{-5}$ cm/s. The majority of compounds have MDCK cell permeability value > 2.10^{-5} cm/s which indicates that they have passive MDCK cell permeability. The HIA % is ranging from 0.008 to 0.118 which means a good oral bioavailability for all the studied compounds.

The physicochemical properties of tested compounds represented in Table S-2 shows that they have a good pharmacokinetic profile and can be considered drug candidates since there are zero Lipinski property violations. The bioactivity study shows that all the studied compounds have negative value, indicating low affinity and suggesting they are not mutagenic or tumorigenic. Except for ICM value, compounds **2a**, **2b** and **4a** have positive values: 0.42, 0.36 and 0.54 respectively. This suggests that these three compounds may modulate ion channels (channel blockers or channel openers).

3. 5. Multilinear Regression (MLR).

Due to the limited number of IC_{50} values for the molecules studied in the present work (see Table 2), the MLR results should be treated as preliminary, and nevertheless several conclusions can be drawn. Correlation analysis revealed that the relationship between (IP + PDE), PA, and ETE descriptor calculated in water for the studied benzofuran derivatives at the

B3LYP/6-311G level of theory, and experimental IC_{50} [23] data gives the best following multilinear regression:



Histogram 2: PPB% affinity as vs. compounds.

$$IC_{50}(\mu M) = 0.563 + 148.25 * (IP + PDE) - 148.42 * PA - 147.89 * ETE$$
(6)

with a squared correlation coefficient equal to 0.99 and with a critical value of Fisher index (F) equal to 0.08; F-value is found statistically significant at 95% level. The same qualitative relation is obtained at B3LYP/6-311G(d, p) with a squared correlation coefficient equal to 0.95, and with a critical value of Fisher index equal to 0.3.

Cheng and Prusoff,⁴⁸ showed that the IC₅₀ of an enzyme inhibitor is proportional to its inhibition constant Ki. Therefore, the affinity of an inhibitor is higher when the Ki, and the IC₅₀ are small. If the predicted IC₅₀ values (calculated with relation 6) within the context of the MLR model (see Table 5) are considered under the same operating conditions, it emerges that molecules **1b** (7.81), **3f** (8.36), and **4d** (8,17 μ M) exhibit IC₅₀ values close to the reference (Trolox with 5.21 μ M). The relative average error is 2.1% (see table 5). This indicated values for our new molecules are accurate.

Table 5: (IC₅₀) and relative error obtained with relation (6).

Compounds	IC ₅₀ (μM) (LMR)	IC ₅₀ (exp) (exp) (μM)	Relative error in %*
Trolox	5.21	5.42	4
1b	7.81	/	/
2a	10.39	/	/
2b	10.28	/	/
3a	16.83	/	/
3b	9.62	/	/
3c	10.27	10.59	3
3d	9.72	9.72	0
3e	8.47	/	/
3f	8.36	8.57	2.5
4a	8.54	/	/
4b	9.39	/	/
4c	11.23	/	/
4d	8.17	8.27	1.2
4e	10.07	/	/
4f	11.55	/	/

*Relative error % = $\frac{|IC50(LMR) - IC50(exp)|}{IC50(exp)} \cdot 100$

4. Conclusion

The antioxidant activity of benzofuran Schiff base derivatives and benzofuran thiazolidinone derivatives was evaluated using DFT calculations. Different molecular descriptors, associated with the antioxidant activity, were calculated. Our results indicate that khellin (1a) is not a good antioxidant, but its enol form (1b) was found to be more potent than Trolox. The two hydrolyzed derivatives of khellin (2a) and (2b) exhibited moderate antioxidant activity. The results also indicate also that benzofuran thiazolidinone derivatives (4a-4f) are better antioxidants than benzofuran Schiff base derivatives (3a-3f), which is in

good agreement with experimental results. From BDEs,3c and 4d are the most active among the studied benzofuran derivatives independent of the media, while 3f and 4a are the poorest. From IPs values, 3a, 3f, and 4d are a good electron-donating than in the four others environment, while 3c, 3e, and 4c are the least effective. From PAs, 3a and 4e are more prone to deprotonation than others.

Comparing the parameters reported in Tables 2, S-1, 4, and S-2, the BDEs values are significantly lower than the IPs and PAs in the gas and in benzene solution. In the gas phase and non-polar solvents, the HAT process is likely to be favorable than SET-PT and SPLET. In the studied environments, the calculated IPs, for all the benzofuran derivatives, are significantly higher than the BDEs and Pas in all cases except for water where IPs values are lower than BDEs but higher than the Pas values. Thus, the SET-PT mechanism is the least favored indifferent solvents. PAs values decrease and become significantly lower than BDEs and IPs in DMSO and aqueous solutions when the polarity of the solvent increases, which makes SPLET favorable in polar environment.

The BDEs of the unsubstituted benzofuran derivatives, when compared, indicate that electron-withdrawing groups (EWG) attached to π conjugated groups at the N position decrease BDEs. However, electron-donating groups (EDG) reduce BDEs values. Thus, EDG is useful to decrease the IPs values, which increases the electron-donating ability of the studied benzofuran derivatives. In contrast, the EWG process decreases the PAs values and increases the deprotonation. Notably, in each environment (gas or solvated phases), (IP+PDE) and (PA+ETE) are perfectly correlated with BDE. The above results, rationalize the antioxidant effect of these benzofuran derivatives, providing valuable information for the design and synthesis of a new powerful antioxidant.

5. References

 E. G. Rogan, E. L. Cavalleri, Oxidative Stress: Diagnostics, Prevention, and Therapy, Chapter 4, 83–98, Editor(s) S. Andreescu, M. Hepel, ACSSymposium Series. 2011.

DOI:10.1021/bk-2011-1083.ch004

2. M. Valko, D. Leibfritz, J. Moncol, M. T. D. Cronin, M. Mazur, J. Telser, *Int. J. Biochem. Cell. Biol.* **2007**, *39*, 44–84.

DOI:10.1016/j.biocel.2006.07.001

- Y. Z. Fang, S. Yang, G. Wu, Nutr. 2002, 18, 872–879
 DOI:10.1016/S0899-9007(02)00916-4
- a. K. L. Fritz, C. M. Seppanen, M. S. Kurzer, A. Csallany Saari, Nutr. Res. 2003, 23, 479–487.

DOI:10.1016/S0271-5317(03)00005-8

b. S. Hachemaoui, T. E. A. Ardjani, H. Brahim, J. R. Alvarez-Idaboy, *J. Mol. Model.* **2024**, *30*, 205.

DOI:10.1007/s00894-024-06010-2

- P. I. Oteiza, A. G. Erlejman, S. V. Verstraeten, C. L. Keen, C. G. Fraga, Clin. Dev. Immunol. 2005, 12, 19–25.
 DOI:10.1080/10446670410001722168
- H. Khanam, S. M. Shamsuzzaman, Eur. J. Med. Chem. 2015, 97, 483–504. DOI:10.1016/j.ejmech.2014.11.039
- S. Narimatsu, C. Takemi, S. Kuramoto, D. Tsuzuki, H. Hichi-ya, K. Tamagake, S. Yamamoto, *Chirality* 2003, 15, 333–339.
 DOI:10.1002/chir.10212
- H. C. Cheng, C. M. Ulane, R. E. Burke, Ann. Neurol. 2010, 67, 715–725. DOI:10.1002/ana.21995
- J. C. González-Gómez, L. Santana, E. Uriarte, *Tetrahedron*.
 2005, 61, 4805–4810. DOI:10.1016/j.tet.2005.03.018
- M. Koca, S. Servi, C. Kirilmis, M. Ahmedzade, C. Kazaz, B. Ozbek, G. Otük, *Eur. J. Med. Chem.* 2005, 40, 1351–1358.
 DOI:10.1016/j.ejmech.2005.07.004
- 11. C. L. Kao, J. W. Chern, *Tetrahedron Lett.* **2001**, *42*, 1111–1113. **DOI:**10.1016/S0040-4039(00)02163-8
- 12. R. Naik, D. S. Harmalkar, X. Xu, K. Jang, K. Lee, *Eur. J. Med. Chem.* **2015**, *90*, 379–393. **DOI:**10.1016/j.ejmech.2014.11.047
- S. He, P. Jain, B. Lin, M. Ferre, Z. Hu, ACS. Comb. Sci. 2015,17, 641–652. DOI:10.1021/acscombsci.5b00101
- A. Verma, S. K. Saraf, Eur. J. Med. Chem. 2008,43, 897–905.
 DOI:10.1016/j.ejmech.2007.07.017
- A. C. Tripathi, S. J. Gupta, G. N. Fatima, P. K. Sonar, A. Verma, S. K. Saraf, *Eur. J. Med. Chem.* **2014**, *72*, 52–77.
 DOI:10.1016/j.ejmech.2013.11.017
- 16. D. P. Gouvea, F. A. Vasconcellos, G. dos AnjosBerwaldt, A. C. Pinto Seixas Neto, G. Fischer, R. P. Sakata, W. P. Almeida, W. Cunico, *Eur. J. Med. Chem.* 2016, 118, 259–265. DOI:10.1016/j.ejmech.2016.04.028
- M. L. Barreca, J. Balzarini, A. Chimirri, E. De Clercq, L. De Luca, H. D. Höltje, *J. Med. Chem.* 2002, 45, 5410–5413.
 DOI:10.1021/jm020977
- A. Rao, J. Balzarini, A. Carbone, A. Chimirri, E. De Clercq,
 A. M. Monforte, P. Monforte, C. Pannecouque, M. Zappalà,
 Antiviral. Res. 2004, 63, 79–84.
 - DOI:10.1016/j.antiviral.2004.03.004
- R. K. Rawal, R. Tripathi, S. B. Katti, C. Pannecouque, E. De Clercq, *Bioorganic. Med. Chem.* 2007, *15*, 3134–3142.
 DOI:10.1016/j.bmc.2007.02.044
- 20. L. R. Pessoa de Siqueira, P. A. Teixeira de Moraes Gomes, L. Pelagia de Lima Ferreira, M. J. Barreto de Melo Rêgo, A. C. Lima Leite, *Eur. J. Med. Chem.* 2019, 170, 237–260. DOI:10.1016/j.ejmech.2019.03.024
- O. A. El-khouly, M. A. Henen, M. A. El-sayed, M. I. Shabaan,
 S. M. El-messery, *Bioorg. Med. Chem.* 2021, 1, 31, 115976.
 DOI:10.1016/j.bmc.2020.115976
- J. R. Hwu, N. K. Gupta, S. C. Tsay, W. C. Huang, I. C. Albulescu, K. Kovacikova, M. J. Van Hemert, *Antivira. Res.* 2017, 46, 96–101. DOI:10.1016/j.antiviral.2017.08.008
- N. A. Abdel Latif, Ah. H. Abdel Hafez, L. M. Break, Russ. J. Bioorganic. Chem. 2013, 39, 438–443.
 DOI:10.1134/S106816201304002X
- K. Chand, A. Hiremathad, M. Singh, M. A. Santos, R. S. Keri, *Phamacol. Rep.* 2016, 69, 281–295.
 DOI:10.1016/j.pharep.2016.11.007

- F. Ati, A. Chergui, H. Y. Aboul-Enein, B. Maouche, *Egypt. Pharm. J.* 2018, *17*, 212–217. DOI:10.4103/ejo.ejo_31_17
- 26. M. J. Frisch, G. W. Trucks, H. B. Schlegel, G. E. Scuseria, M. A. Robb, et al., **2009**, Gaussian 09 Revision A.2.
- A. D. Becke, J. Chem. Phys. 1993, 98, 5648–5652.
 DOI:10.1063/1.464913
- C. Lee, W. Yang, R. G. Parr, Phys. Rev. B. Condens. Matter. 1988, 37, 785–789. DOI:10.1103/PhysRevB.37.785
- J. Tomasi, B. Mennucci, R. Cammi, Chem. Rev. 2005, 105, 2999–3093. DOI:10.1021/cr9904009
- V. Barone, M. Cossi, J. Tomasi, J. Chem. Phys. 1997, 107, 3210–3221. DOI:10.1063/1.474671
- 31. a) G. Xiong, Z. Wu, J. Yi, L. Fu, Z. Yang, C. Hsieh, M. Yin, X. Zeng, C. Wu, A. Lu, X. Chen, T. Hou, D. Cao, *Nucleic. Acids. Res.* **2021**, *9*(W1), W5–W14. **DOI:**10.1093/nar/gkab255 b) https://admetmesh.scbdd.com.
- 32. To calculate bioactivity online properties, http://www.molinspiration.com
- 33. A. Galano, *J. Mex. Chem. Soc.* **2015**, *59*, 231–262. https://www.scielo.org.mx/scielo.php?script=sci_arttext&pid=S1870-249X2015000400002
- 34. M. Leopoldini, N. Russo, M. Toscano, *Food. Chem.* **2011**, *125*, 288–306. **DOI**:10.1016/j.foodchem.2010.08.012
- 35. G. Wang, Y. Liu, L. Zhang, L. An, R. Chen, Y. Liu, Q. Luo, Y. Li, H. Wang, Y. Xue, *Food. Chem.* 2020,304, 125446. DOI:10.1016/j.foodchem.2019.125446
- 36. J. S. Wright, E. R. Johnson, G. A. Dilabio, *J. Am. Chem. Soc.* **2001**, *123*, 1173–1183. **DOI**:10.1021/ja002455u
- D. Amić, V. Stepanić, B. Lučić, Z. Marković, J. M. Dimitrić Marković, J. Mol. Model. 2013, 19, 2593–603.
 DOI:10.1007/s00894-013-1800-5
- K. M. Schaich, X. Tian, J. Xie, J. Funct. Foods. 2015, 14, 111–125. DOI:10.1016/j.jff.2015.01.043
- M. C. Foti, J. Agric. Food. Chem. 2015, 63, 8765–8776.
 DOI:10.1021/acs.jafc.5b03839
- G. Buemi, 2006. Intramolecular Hydrogen Bonds. Methodologies and Strategies for Their Strength Evaluation. In: Grabowski, S. J. (eds) Hydrogen Bonding—New Insights., vol 3. Springer, Dordrecht.
 DOI:10.1007/978-1-4020-4853-1_2
- 41. M. Leopoldini, I. P. Pitarch, N. Russo, M. Toscano, *J. Phys. Chem. A.* **2004**, *108*, 92–96. **DOI**:10.1021/jp035901j
- 42. N. Nenadis, M. Z. Tsimidou, *Food. Res. Int.* **2012**, *48*, 538–543. **DOI:**10.1016/j.foodres.2012.05.014
- Y. Yuan, S. Chang, Z. Zhang, Z. Li, S. Li, P. Xie, W. P. Yau, H. Lin, W. Cai, Y. Zhang, X. Xiang, *Chemom. Intell. Lab. Syst.* 2020,199, 103962. DOI:10.1016/j.chemolab.2020.103962
- 44. N. N Wang, C. Huang, J. Dong, Z. J. Yao, M. F. Zhu, Z. K. Deng, B. Lv, A. P. Lu, A. F. Chen, D. S. Cao, *RSC. Adv.* **2017**, *7*, 19007–19018. **DOI:**10.1039/C6RA28442F
- B. Shaker, M. S. Yu, J. S. Song, S. Ahn, J. Y. Ryu, K. S. Oh, D. Na, *Bioinformatics* 2021, 37, 1135–1139.
 DOI:10.1093/bioinformatics/btaa918
- J. D. Irvine, L. Takahashi, K. Lockhart, J. Cheong, J. W. Tolan, H. E. Selick, J. R. Grove, *J. Pharm. Sci.* 1999, 88, 28–33.
 DOI:10.1021/js9803205

 J. Bockaert, S. Claeysen, C. Bécamel, S. Pinloche, A. Dumuis, *Int. Rev. Cytol.* 2002, 212, 63–132.
 DOI:10.1016/S0074-7696(01)12004-8 48. Y. C. Cheng, W. H. Prusoff, Biochemical. *Pharmacol.* **1973**, 22, 3099–3108. **DOI**:10.1016/0006-2952(73)90196-2

Povzetek

Raziskali smo sposobnost benzofuranskih Schiffovih baz in tiazolidinonskih derivatov za lovljenje prostih radikalov, pri čemer smo uporabili kvantno kemijski računski pristop na osnovi teorije gostotnega funkcionala (DFT). Obravnavali smo tri glavne mehanizme: zaporedno izgubo protona in prenos elektrona (SPLET), prenos enega elektrona, ki mu sledi prenos protona (SET-PT), ter prenos vodikovega atoma (HAT). Za te mehanizme smo izračunali različne termodinamske količine v modelu izoliranega sistema ter v implicitno modeliranem topilu na ravni teorije B3LYP/6-311G in 6-311G(d,p). Naše ugotovitve kažejo, da spojine 3a, 3c, 3f, 4d in 4e zajemajo proste radikale prek enega od teh treh mehanizmov. Rezultati potrjujejo, da SPLET prevladuje v polarnih okoljih, medtem ko HAT predstavlja termodinamsko najugodnejši mehanizem v plinski fazi in nepolarnih raztopinah. Elektron-privlačne skupine (EWG), vezane na π -konjugirani sistem na N-položaju benzofuranskih derivatov zmanjšujejo entalpijo disociacije vezi (BDE), medtem ko elektron-donorske skupine (EDG) znižujejo ionizacijske potenciale (IP). Statistična analiza z multiplo linearno regresijo kaže na močno povezavo med IC50 in ionizacijskim potencialom ter entalpijo disociacije protona, protonsko afiniteto in entalpijo prenosa elektrona.



Except when otherwise noted, articles in this journal are published under the terms and conditions of the Creative Commons Attribution 4.0 International License